



SAKARYA ÜNİVERSİTESİ

FEN BİLİMLERİ ENSTİTÜSÜ DERGİSİ

Sakarya University Journal of Science
SAUJS

ISSN 1301-4048 | e-ISSN 2147-835X | Period Bimonthly | Founded: 1997 | Publisher Sakarya University |
<http://www.saujs.sakarya.edu.tr/>

Title: Investigation of Lateral and Vertical Dynamic Responses of a Full Car Model
Exposed to Sine Road Input

Authors: Mustafa EROĞLU

Received: 2022-05-23 00:00:00

Accepted: 2022-06-28 00:00:00

Article Type: Research Article

Volume: 26

Issue: 4

Month: August

Year: 2022

Pages: 829-841

How to cite

Mustafa EROĞLU; (2022), Investigation of Lateral and Vertical Dynamic Responses
of a Full Car Model Exposed to Sine Road Input. Sakarya University Journal of
Science, 26(4), 829-841, DOI: 10.16984/saufenbilder.1120433

Access link

<http://www.saujs.sakarya.edu.tr/en/pub/issue/72361/1120433>

New submission to SAUJS

<http://dergipark.gov.tr/journal/1115/submission/start>

Investigation of Lateral and Vertical Dynamic Responses of a Full Car Model Exposed to Sine Road Input

Mustafa EROĞLU*¹

Abstract

In this study, the full car model, which is exposed to a sinusoidal road input, has been examined to ensure the driving safety of the vehicles and the comfort of the passengers. In this context, the full car, including lateral and vertical movements, is modeled with fourteen degrees of freedom. The second-order equations of motion of the modeled vehicle were obtained using the Lagrangian method and reduced to first-order equations of motion using the state-space form. Then, these equations of motion were solved precisely in the time domain using the Euler method in the Matlab environment. To examine the lateral movements and the rotations of the vehicle in the pitch and roll axis, a sine wave with a wavelength of 5 m and an amplitude of 0,1 m was applied to the wheels of the vehicle. In the analysis, the right front wheel is exposed to a sinusoidal road input at $t=0$ s, while the left front wheel is exposed to a sinusoidal road input after the vehicle moves 2,5 m. Thus, both the pitch and roll motion of the vehicle will be examined in detail. In the study, four different vehicle masses 500 kg, 1000 kg, 2000 kg, and 3000 kg were taken into consideration and the effect of different vehicle masses on passenger and vehicle dynamic behaviors was investigated. In addition, the situation of passing vehicles at variable speeds from the given disruptive road input has also been examined. The maximum dynamic responses of the passenger and the vehicle were examined when the vehicle speed changed from 3 m/s to 50 m/s by 0,1 m/s. In the study, it has been observed that the vehicle mass and certain vehicle speed have effects on the vertical and lateral displacements and accelerations of the passenger and the vehicle.

Keywords: Full car model, passive suspension system, ride holding, passenger comfort

1. INTRODUCTION

Vehicle suspension systems are mechanical systems positioned between the wheels and the vehicle body to minimize the vertical vibrations of vehicles exposed to disruptive road inputs. The performance

of the suspension systems is important in terms of vehicle driving dynamics and the comfort of the passengers carried. The main purpose of suspension systems consisting of spring, damping elements, and connection equipment is to ensure the driving safety of the vehicle and the comfort of the passengers.

* Corresponding author: mustafaeroglu@sakarya.edu.tr

¹ Sakarya University

ORCID: <https://orcid.org/0000-0002-1429-7656>

It is expected that both driving safety and passenger comfort will give the highest performance in vehicles. However, it is very difficult for both of them to give maximum performance in passive suspension systems. Because driving safety and passenger comfort are parameters that affect each other. Traditionally, passive suspension systems used in many vehicles have only spring and damping elements, and their coefficients are fixed but cannot be changed. In passive suspensions, there are semi-active and active suspensions that allow for external control. Within the scope of simulation and analysis of suspension systems, Agarkakli et al. performed the passive and active suspension analysis of the quarter car model exposed to different road inputs [1]. Again, using the quarter car model, Nagarkar et al. made optimization and control in Matlab/Simulink environment with PID and LQR controller [2].

Yildirim and Esen examined the dynamic behavior in the vertical direction only by using a full vehicle model, taking into account different road inputs and different vehicle speeds [3]. The most used controller as an active controller in vehicle suspension systems is usually fuzzy logic. Yagiz et al. studied the active suspension control of a five-degree-of-freedom car model using fuzzy logic [4]. Salem and Aly proposed an active suspension system to ensure the driving comfort of the quarter car, which was modeled as two degrees of freedom using a fuzzy logic controller [5]. Fuzzy logic controllers and PID type controllers are used as a hybrid. In this context, Singh and Aggarwal controlled the passenger seat vibrations of the semi-active quarter car model using hybrid fuzzy logic and the PID approach [6]. Again, the same author reduced the vibrations of a three-degree-of-freedom quarter-car by using fuzzy logic and a self-adaptive fuzzy logic controller modeled as a hybrid [7]. Swethamarai and Lakshmi designed a hybrid fuzzy logic and PID controller in the active quarter car model to minimize the vibrations affecting the driver [8].

Eroğlu et al. investigated the dynamic responses of the car using a fuzzy logic controller with PID in the

car-bridge interaction model using a quarter car [9]. In some studies, bridges where high-speed trains pass have been modeled as Euler-Bernoulli beams and analyzed [10].

In the literature, it has been seen that vehicle models are generally modeled as quarter models for convenience. In some studies, controllers such as H_∞ , and LQR have been preferred to minimize the vibrations affecting the vehicle and passenger by using the quarter vehicle model [11-13]. In some studies, the dynamic behavior of bridges modeled as beams without using active controllers has been investigated using a tuned mass damper [14].

In most of the studies given above, car models are generally considered quarter or half models. In addition, almost all studies have examined the dynamic behavior of vehicles only in the vertical direction. In this study, the vehicle model can be modeled as having fourteen degrees of freedom and can be examined in dynamic responses in the lateral direction. With the full vehicle model, dynamic displacements and acceleration values affecting the passenger were examined according to the mass of the vehicle and the speed of the vehicle.

2. FULL CAR MODEL

In this section, the definitions of the full car model exposed to sinus road input will be made. When both lateral and vertical movements of the full car model examined in this study are examined, the full car model is modeled as fourteen degrees of freedom. Fourteen independent degrees of freedom are shown in Figure 1. In addition, a full car model and a passenger seat are also included in the model. Thus, lateral and vertical dynamic behaviors affecting both the passenger and the vehicle can be examined. When the parameters in Figure 1 are examined, the mass of the passenger is represented by m_d , the mass of the vehicle is represented by m_c and the mass of the wheels is represented by m_w . I_{cx} and I_{cy} represent the mass moments of inertia about the roll and pitch axis, respectively. The k_{dz} , c_{dz} , k_{dy} and k_{dy} parameters represent the vertical and lateral

suspension coefficients between the passenger seat and the vehicle, respectively. While k_{w1z} , k_{w2z} , k_{w3z} and k_{w4z} represent the stiffness coefficients in the vertical direction between the vehicle and the wheel, k_{w1y} , k_{w2y} , k_{w3y} and k_{w4y} represent the lateral stiffness coefficients. Similarly, c_{w1z} , c_{w2z} , c_{w3z} , and c_{w4z} represent the damping coefficient in the vertical direction, while c_{w1y} , c_{w2y} , c_{w3y} , and c_{w4y} represent the damping coefficient in the lateral direction. The parameters k_{r1} , k_{r2} , k_{r3} , and k_{r4} represent the stiffness coefficient of the tire. r_{dz} and r_{dy} describe the vertical and lateral displacement of the passenger, respectively, while r_{cz} and r_{cy} describe the vertical and lateral displacements of the vehicle. While r_{w1z} , r_{w2z} , r_{w3z} , and r_{w4z} describe the movement of the wheels in the vertical direction, r_{w1y} , r_{w2y} , r_{w3y} and r_{w4y} describe their movement in the lateral direction. In addition, the roll and pitch movements of the vehicle are represented by θ_{cx} and θ_{cy} . r_1 , r_2 , r_3 , and r_4 represent the sinusoidal effect coming from the

road to the wheels. Distances a and b define the length of the vehicle's center of mass to the front and rear wheels, respectively, while distances c and d define the distance to the right and left wheels. The lengths e and f define the distances from the passenger seat to the center of mass of the vehicle. The values of all given parameters are shown in Table 1.

To examine the dynamic responses of the full car model, it is necessary to obtain the equations of motion for each degree of freedom. In this study, the Lagrangian method was used to obtain the equations of motion. The kinetic energy, potential energy, and damping function of the full car model are given in Equations (1-3).

Using equation (1-3), the Lagrangian expression can be written as follows. The generalized coordinates of the full car model are taken as in Equation 5.

$$E_k = \frac{1}{2} \left[m_d \dot{r}_{dz}^2 + m_d \dot{r}_{dy}^2 + m_c \dot{r}_{cz}^2 + m_c \dot{r}_{cy}^2 + I_{cx} \dot{\theta}_{cx}^2 + I_{cy} \dot{\theta}_{cy}^2 + m_w \dot{r}_{w1z}^2 + m_w \dot{r}_{w2z}^2 + m_w \dot{r}_{w3z}^2 + m_w \dot{r}_{w4z}^2 + m_w \dot{r}_{w1y}^2 + m_w \dot{r}_{w2y}^2 + m_w \dot{r}_{w3y}^2 + m_w \dot{r}_{w4y}^2 \right] \quad (1)$$

$$E_p = \frac{1}{2} \left[k_{dz} [r_{dz} - r_{cz} + \theta_{cy} e - \theta_{cx} f]^2 + k_{dy} [r_{dy} - r_{cy} + \theta_{cx} h]^2 + k_{w1z} [r_{cz} - r_{w1z} - \theta_{cy} a - \theta_{cx} c]^2 + k_{w2z} [r_{cz} - r_{w2z} - \theta_{cy} a + \theta_{cx} d]^2 + k_{w3z} [r_{cz} - r_{w3z} + \theta_{cy} b - \theta_{cx} c]^2 + k_{w4z} [r_{cz} - r_{w4z} + \theta_{cy} b + \theta_{cx} d]^2 + k_{w1y} [r_{cy} - r_{w1y}]^2 + k_{w2y} [r_{cy} - r_{w2y}]^2 + k_{w3y} [r_{cy} - r_{w3y}]^2 + k_{w4y} [r_{cy} - r_{w4y}]^2 + k_{r1} [r_{w1z} - r_1]^2 + k_{r2} [r_{w2z} - r_2]^2 + k_{r3} [r_{w3z} - r_3]^2 + k_{r4} [r_{w4z} - r_4]^2 \right] \quad (2)$$

$$D = \frac{1}{2} \left[c_{dz} [\dot{r}_{dz} - \dot{r}_{cz} + \dot{\theta}_{cy} e - \dot{\theta}_{cx} f]^2 + c_{dy} [\dot{r}_{dy} - \dot{r}_{cy} + \dot{\theta}_{cx} h]^2 + c_{w1z} [\dot{r}_{cz} - \dot{r}_{w1z} - \dot{\theta}_{cy} a - \dot{\theta}_{cx} c]^2 + c_{w2z} [\dot{r}_{cz} - \dot{r}_{w2z} - \dot{\theta}_{cy} a + \dot{\theta}_{cx} d]^2 + c_{w3z} [\dot{r}_{cz} - \dot{r}_{w3z} + \dot{\theta}_{cy} b - \dot{\theta}_{cx} c]^2 + c_{w4z} [\dot{r}_{cz} - \dot{r}_{w4z} + \dot{\theta}_{cy} b + \dot{\theta}_{cx} d]^2 + c_{w1y} [\dot{r}_{cy} - \dot{r}_{w1y}]^2 + c_{w2y} [\dot{r}_{cy} - \dot{r}_{w2y}]^2 + c_{w3y} [\dot{r}_{cy} - \dot{r}_{w3y}]^2 + c_{w4y} [\dot{r}_{cy} - \dot{r}_{w4y}]^2 \right] \quad (3)$$

$$\frac{d}{dt} \left(\frac{\partial L}{\partial \dot{\eta}_k(t)} \right) - \frac{\partial L}{\partial \eta_k(t)} + \frac{\partial D}{\partial \dot{\eta}_k(t)} = 0 \quad k = 1, 2, 3 \dots 14 \quad (4)$$

$$\boldsymbol{\eta}(t) = \begin{Bmatrix} r_{dz} & r_{dy} & r_{cz} & r_{cy} & \theta_{cy} & \theta_{cx} & r_{w1z} & r_{w2z} \\ r_{w3z} & r_{w4z} & r_{w1y} & r_{w2y} & r_{w3y} & r_{w4y} \end{Bmatrix}^T, \quad (5)$$

Using the Lagrangian method, the fourteen equations of motion of the full car model are obtained as follows.

Vertical displacement of the passenger:

$$m_d \ddot{r}_{dz} + k_{dz} [r_{dz} - r_{cz} + \theta_{cy} e - \theta_{cx} f] + c_{dz} [\dot{r}_{dz} - \dot{r}_{cz} + \dot{\theta}_{cy} e - \dot{\theta}_{cx} f] = 0 \quad (6)$$

Lateral displacement of the passenger:

$$m_d \ddot{r}_{dy} + k_{dy} [r_{dy} - r_{cy} + \theta_{cx} h] + c_{dy} [\dot{r}_{dy} - \dot{r}_{cy} + \dot{\theta}_{cx} h] = 0 \quad (7)$$

Vertical displacement of the car body:

$$\begin{aligned} m_c \ddot{r}_{cz} - k_{dz} [r_{dz} - r_{cz} + \theta_{cy} e - \theta_{cx} f] + k_{w1z} [r_{cz} - r_{w1z} - \theta_{cy} a - \theta_{cx} c] \\ + k_{w2z} [r_{cz} - r_{w2z} - \theta_{cy} a + \theta_{cx} d] + k_{w3z} [r_{cz} - r_{w3z} + \theta_{cy} b - \theta_{cx} c] \\ + k_{w4z} [r_{cz} - r_{w4z} + \theta_{cy} b + \theta_{cx} d] - c_{dz} [\dot{r}_{dz} - \dot{r}_{cz} + \dot{\theta}_{cy} e - \dot{\theta}_{cx} f] \\ + c_{w1z} [\dot{r}_{cz} - \dot{r}_{w1z} - \dot{\theta}_{cy} a - \dot{\theta}_{cx} c] + c_{w2z} [\dot{r}_{cz} - \dot{r}_{w2z} - \dot{\theta}_{cy} a + \dot{\theta}_{cx} d] \\ + c_{w3z} [\dot{r}_{cz} - \dot{r}_{w3z} + \dot{\theta}_{cy} b - \dot{\theta}_{cx} c] + c_{w4z} [\dot{r}_{cz} - \dot{r}_{w4z} + \dot{\theta}_{cy} b + \dot{\theta}_{cx} d] = 0 \end{aligned} \quad (8)$$

Lateral displacement of the car body:

$$\begin{aligned} m_c \ddot{r}_{cy} - k_{dy} [r_{dy} - r_{cy} + \theta_{cx} h] + k_{w1y} [r_{cy} - r_{w1y}] + k_{w2y} [r_{cy} - r_{w2y}] \\ + k_{w3y} [r_{cy} - r_{w3y}] + k_{w4y} [r_{cy} - r_{w4y}] - c_{dy} [\dot{r}_{dy} - \dot{r}_{cy} + \dot{\theta}_{cx} h] \\ + c_{w1y} [\dot{r}_{cy} - \dot{r}_{w1y}] + c_{w2y} [\dot{r}_{cy} - \dot{r}_{w2y}] \\ + c_{w3y} [\dot{r}_{cy} - \dot{r}_{w3y}] + c_{w4y} [\dot{r}_{cy} - \dot{r}_{w4y}] = 0 \end{aligned} \quad (9)$$

Pitch motion of the car body:

$$\begin{aligned} I_{cy} \ddot{\theta}_{cy} + k_{dz} e [r_{dz} - r_{cz} + \theta_{cy} e - \theta_{cx} f] - k_{w1z} a [r_{cz} - r_{w1z} - \theta_{cy} a - \theta_{cx} c] \\ - k_{w2z} a [r_{cz} - r_{w2z} - \theta_{cy} a + \theta_{cx} d] + k_{w3z} b [r_{cz} - r_{w3z} + \theta_{cy} b - \theta_{cx} c] \\ + k_{w4z} b [r_{cz} - r_{w4z} + \theta_{cy} b + \theta_{cx} d] + c_{dz} e [\dot{r}_{dz} - \dot{r}_{cz} + \dot{\theta}_{cy} e - \dot{\theta}_{cx} f] \\ - c_{w1z} a [\dot{r}_{cz} - \dot{r}_{w1z} - \dot{\theta}_{cy} a - \dot{\theta}_{cx} c] - c_{w2z} a [\dot{r}_{cz} - \dot{r}_{w2z} - \dot{\theta}_{cy} a + \dot{\theta}_{cx} d] \\ + c_{w3z} b [\dot{r}_{cz} - \dot{r}_{w3z} + \dot{\theta}_{cy} b - \dot{\theta}_{cx} c] + c_{w4z} b [\dot{r}_{cz} - \dot{r}_{w4z} + \dot{\theta}_{cy} b + \dot{\theta}_{cx} d] = 0 \end{aligned} \quad (10)$$

Roll motion of the car body:

$$\begin{aligned}
& I_{cx} \ddot{\theta}_{cx} - k_{dz} f [r_{dz} - r_{cz} + \theta_{cy} e - \theta_{cx} f] - k_{w1z} c [r_{cz} - r_{w1z} - \theta_{cy} a - \theta_{cx} c] \\
& + k_{w2z} d [r_{cz} - r_{w2z} - \theta_{cy} a + \theta_{cx} d] - k_{w3z} c [r_{cz} - r_{w3z} + \theta_{cy} b - \theta_{cx} c] \\
& + k_{w4z} d [r_{cz} - r_{w4z} + \theta_{cy} b + \theta_{cx} d] - c_{dz} f [\dot{r}_{dz} - \dot{r}_{cz} + \dot{\theta}_{cy} e - \dot{\theta}_{cx} f] \\
& - c_{w1z} c [\dot{r}_{cz} - \dot{r}_{w1z} - \dot{\theta}_{cy} a - \dot{\theta}_{cx} c] + c_{w2z} d [\dot{r}_{cz} - \dot{r}_{w2z} - \dot{\theta}_{cy} a + \dot{\theta}_{cx} d] \\
& - c_{w3z} c [\dot{r}_{cz} - \dot{r}_{w3z} + \dot{\theta}_{cy} b - \dot{\theta}_{cx} c] + c_{w4z} d [\dot{r}_{cz} - \dot{r}_{w4z} + \dot{\theta}_{cy} b + \dot{\theta}_{cx} d] = 0
\end{aligned} \tag{11}$$

Vertical displacement of the right front wheel:

$$\begin{aligned}
& m_w \ddot{r}_{w1z} - k_{w1z} [r_{cz} - r_{w1z} - \theta_{cy} a - \theta_{cx} c] \\
& + k_{r1} [r_{w1z} - r_1] - c_{w1z} [\dot{r}_{cz} - \dot{r}_{w1z} - \dot{\theta}_{cy} a - \dot{\theta}_{cx} c] = 0
\end{aligned} \tag{12}$$

Vertical displacement of the left front wheel:

$$\begin{aligned}
& m_w \ddot{r}_{w2z} - k_{w2z} [r_{cz} - r_{w2z} - \theta_{cy} a + \theta_{cx} d] \\
& + k_{r2} [r_{w2z} - r_2] - c_{w2z} [\dot{r}_{cz} - \dot{r}_{w2z} - \dot{\theta}_{cy} a + \dot{\theta}_{cx} d] = 0
\end{aligned} \tag{13}$$

Vertical displacement of the right rear wheel:

$$\begin{aligned}
& m_w \ddot{r}_{w3z} - k_{w3z} [r_{cz} - r_{w3z} + \theta_{cy} b - \theta_{cx} c] \\
& + k_{r3} [r_{w3z} - r_3] - c_{w3z} [\dot{r}_{cz} - \dot{r}_{w3z} + \dot{\theta}_{cy} b - \dot{\theta}_{cx} c] = 0
\end{aligned} \tag{14}$$

Vertical displacement of the left rear wheel:

$$\begin{aligned}
& m_w \ddot{r}_{w4z} - k_{w4z} [r_{cz} - r_{w4z} + \theta_{cy} b + \theta_{cx} d] \\
& + k_{r4} [r_{w4z} - r_4] - c_{w4z} [\dot{r}_{cz} - \dot{r}_{w4z} + \dot{\theta}_{cy} b + \dot{\theta}_{cx} d] = 0
\end{aligned} \tag{15}$$

Lateral displacement of the right front wheel:

$$m_w \ddot{r}_{w1y} - k_{w1y} [r_{cy} - r_{w1y}] - c_{w1y} [\dot{r}_{cy} - \dot{r}_{w1y}] = 0 \tag{16}$$

Lateral displacement of the left front wheel:

$$m_w \ddot{r}_{w2y} - k_{w2y} [r_{cy} - r_{w2y}] - c_{w2y} [\dot{r}_{cy} - \dot{r}_{w2y}] = 0 \tag{17}$$

Lateral displacement of the right rear wheel:

$$m_w \ddot{r}_{w3y} - k_{w3y} [r_{cy} - r_{w3y}] - c_{w3y} [\dot{r}_{cy} - \dot{r}_{w3y}] = 0 \tag{18}$$

Lateral displacement of the left rear wheel:

$$m_w \ddot{r}_{w4y} - k_{w4y} [r_{cy} - r_{w4y}] - c_{w4y} [\dot{r}_{cy} - \dot{r}_{w4y}] = 0 \tag{19}$$

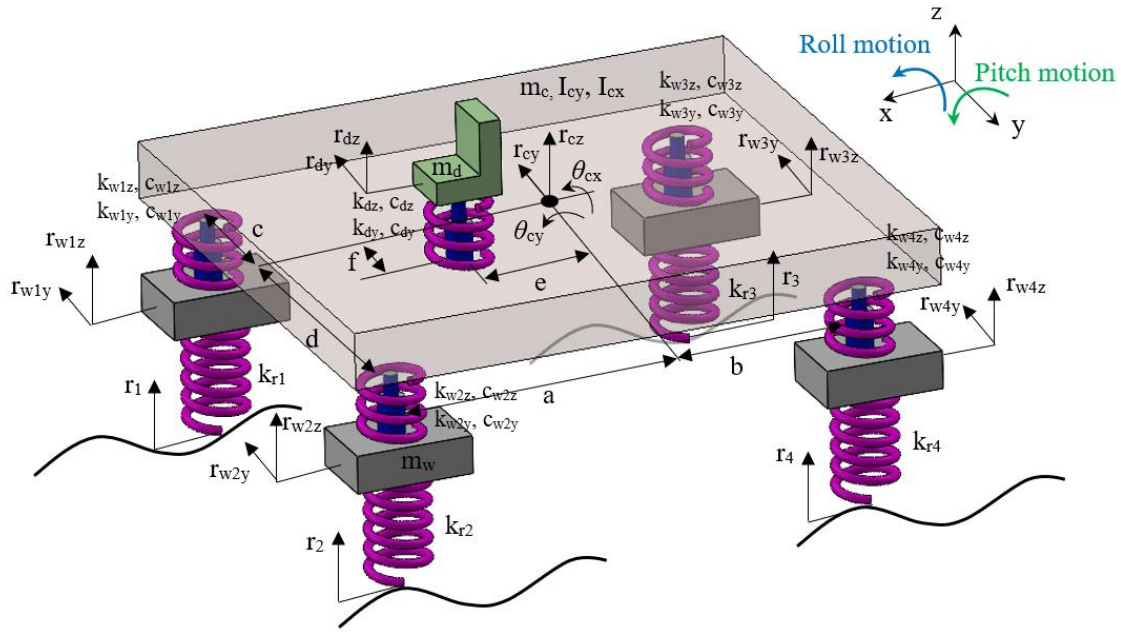


Figure 1 Full car model

The second-order equations of motion of the passengers, vehicles, and wheels in the vertical and lateral directions are given above. The obtained 14 differential equations are reduced to 28 first-order equations of motion by using state-space forms. Thus, when the sinusoidal road input is applied to the

wheels of the full car, as in Figure 2, the dynamic responses of the vehicle and the passenger can be examined in the Matlab program environment by using the Euler method.

Table 1 Full car parameters

<i>Full car model</i>	
Driver mass (m_d)	100 kg
Car mass (m_c)	2000 kg
Wheel mass (m_w)	45 kg
Mass moment of inertia of car around pitch axis (θ_{cy})	1500 kg.m ²
Mass moment of inertia of car around roll axis (θ_{cx})	1680 kg.m ²
Primary suspension stiffness coefficient (k_{dz})	8000 N/m
Primary suspension stiffness coefficient (k_{dy})	14000 /m
Secondary suspension stiffness coefficient ($k_{w1z}, k_{w2z}, k_{w3z}, k_{w4z}$)	25000 N/m
Secondary suspension stiffness coefficient ($k_{w1y}, k_{w2y}, k_{w3y}, k_{w4y}$)	14000 N/m
Tyre stiffness coefficient ($k_{r1}, k_{r2}, k_{r3}, k_{r4}$)	150000 N/m
Primary suspension damping coefficient (c_{dz})	600 Ns/m
Primary suspension damping coefficient (c_{dy})	1600 Ns/m
Secondary suspension damping coefficient ($c_{w1z}, c_{w2z}, c_{w3z}, c_{w4z}$)	1000 Ns/m
Secondary suspension damping coefficient ($c_{w1y}, c_{w2y}, c_{w3y}, c_{w4y}$)	1600 Ns/m
Distance between front wheels and center of the car (a)	1.4 m
Distance between rear wheels and center of the car (b)	1.7 m
Distance between right wheels and center of the car (c)	0,75 m ⁴
Distance between left wheels and center of the car (d)	0.75 m
The vertical distance between driver and center of the car (e)	0.5 m
The lateral distance between driver and center of the car (f)	0.05 m

In this study, the sine input to the car wheels is given using the following formulas

Lateral displacement of the left rear wheel:

$$\begin{aligned}
 r_1 &= 0.1 \sin\left(\pi \frac{vt}{\lambda}\right) & t &\geq 0 \\
 r_2 &= 0.1 \sin\left(\pi \frac{v\left(t - \frac{\lambda}{2v}\right)}{\lambda}\right) & t &\geq \frac{\lambda}{2v} \\
 r_3 &= 0.1 \sin\left(\pi \frac{v\left(t - \frac{a+b}{v}\right)}{\lambda}\right) & t &\geq \frac{a+b}{v} \\
 r_4 &= 0.1 \sin\left(\pi \frac{v\left(t - \frac{a+b+0.5\lambda}{v}\right)}{\lambda}\right) & t &\geq \frac{a+b+0.5\lambda}{v}
 \end{aligned} \tag{20}$$

In Equation 19, the value represented by v represents the car speed and represents the wavelength.

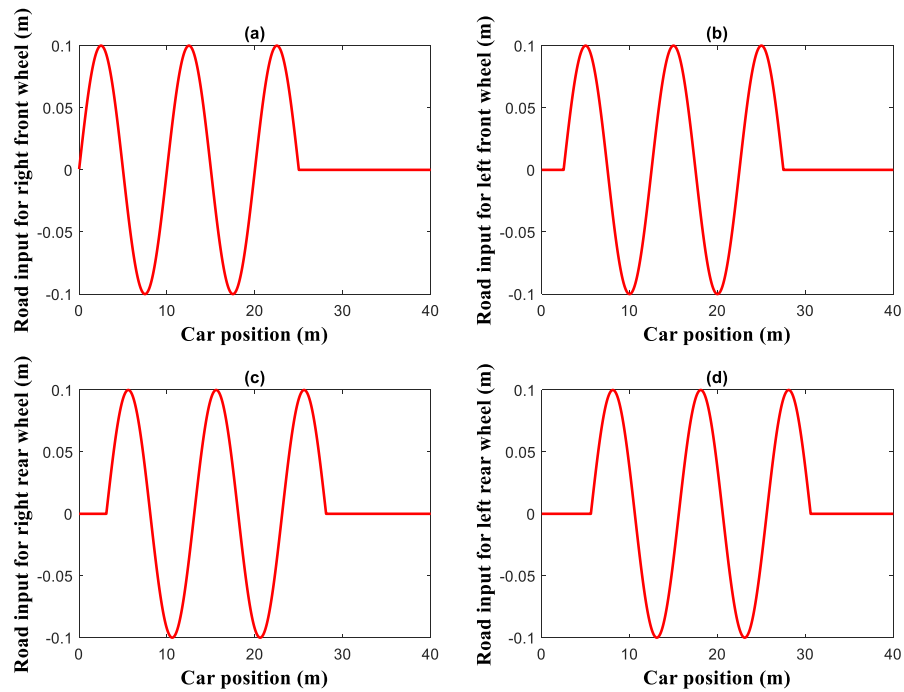


Figure 2 Road input in sine form

3. NUMERICAL SIMULATION

In this study, dynamic behaviors affecting both the vehicle and the passenger will be examined by using a sinusoidal road input. Two different situations were taken into consideration during the analysis. These; the effect of vehicle mass and variable vehicle speed. The road input with a wavelength of 5 m and an amplitude of 0.1 m given in Figure 2 is included in the wheels of the vehicle. When the figure is examined, the front wheels of the vehicle do not enter the disruptive input at the same time. First, the right front wheel is exposed to sinusoidal road input, while the left front wheel is exposed to disruptive road input after passing a distance of half the wavelength. Thus, the rotation of the vehicle around its axes will be examined.

In the analysis, the car speed was taken as a constant 20 m/s. The length of the road input with the sine function is accepted as 25 m. The total analysis time was taken as 6.25 s.

3.1. Effect of Car Mass

In this section, the dynamic responses of the vehicle and the passenger in the vertical and lateral directions will be examined if the vehicle mass is 500 kg, 1000 kg, 2000 kg, and 3000 kg.

In Figure 3 and Figure 4, the displacement and acceleration values of the passenger and the vehicle

in the lateral and vertical directions are given. It can be seen from the graphs that while the vertical displacement of the passenger decrease as the vehicle mass increases, the lateral displacements almost do not change. However, with the increase in vehicle mass, it takes time to dampen the vertical displacements. For example, if the vehicle mass is 500 kg, the vertical displacements are damped when the vehicle travels approximately 60 m, while if the vehicle mass is 3000 kg, the vehicle must move more than 120 m for full damping.

When Figure 3c is examined, the vertical acceleration of the passenger increases to approximately 18 m/s^2 if the vehicle mass is 500 kg, while the maximum vertical acceleration of the passenger is approximately 6 m/s^2 if the vehicle mass is 3000 kg. In other words, with the increase in vehicle mass, the vertical acceleration value decreases 3 times.

When Figure 4 is examined, both the lateral and vertical dynamic responses of the vehicle decrease with the increase in vehicle mass. The vertical displacement graphs of the vehicle in Figure 4a are similar to those in Figure 3a. Similarly, according to the vertical acceleration graph of the vehicle, the acceleration of the vehicle decrease 3 times as the vehicle mass increases. In addition, the lateral dynamic responses of the vehicle in Figure 4 are also highly affected by the vehicle mass.

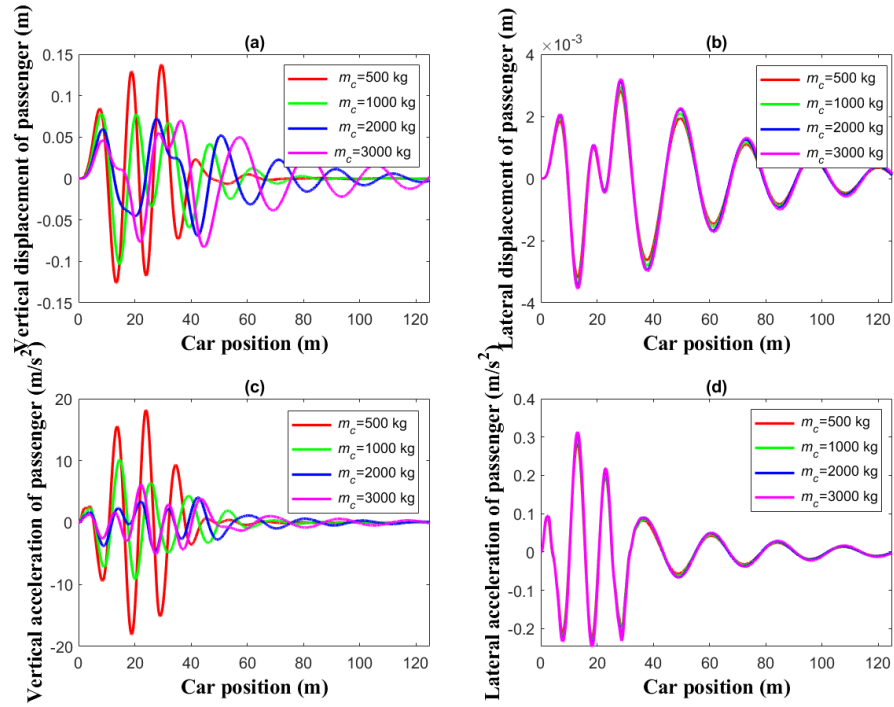


Figure 3 The effect of vehicle mass on the dynamic responses of the passenger in the lateral and vertical directions

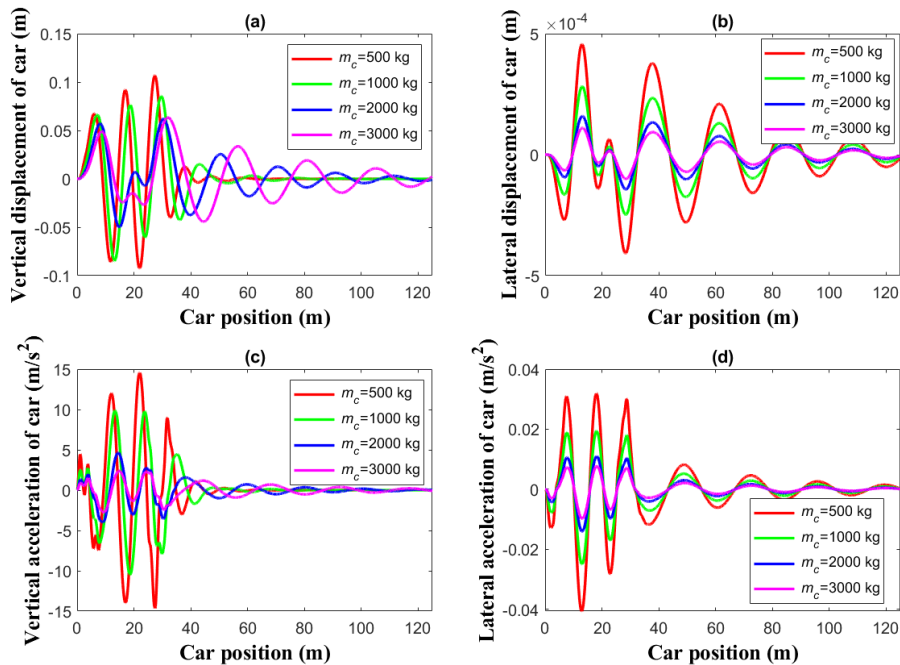


Figure 4 The effect of vehicle mass on the dynamic responses of the car in the lateral and vertical directions

3.2. Effect of Variable Car Velocity

In this section, the situation of the car passing over the sinus road profile at different speeds is examined. In Figure 5-7, when the vehicle changes from 3 m/s to 50 m/s in 0.1 m/s intervals, the maximum lateral and vertical displacements and acceleration values are examined.

When Figure 5 is examined, the maximum dynamic responses of the passenger in the vertical direction occur when the vehicle speed is about 10 m/s, while the maximum dynamic responses in the lateral direction occur when the vehicle speed is about 9 m/s. In all

graphs, the maximum displacement and acceleration of the passenger decrease as the vehicle speed exceed 10 m/s. The lateral and vertical displacement and acceleration graphs of the vehicle in Figure 6 are quite similar to the ones in Figure 5. However, in Figure 6c, it is seen that the vertical acceleration value of the vehicle increases when the vehicle speed exceeds 27 m/s. In addition, the maximum vertical acceleration values affecting the passenger and the vehicle exceed the uncomfortable acceleration value that affects the human being. The uncomfortable acceleration value affecting the human is 0.49 m/s^2 according to the ISO 2631 standard [15].

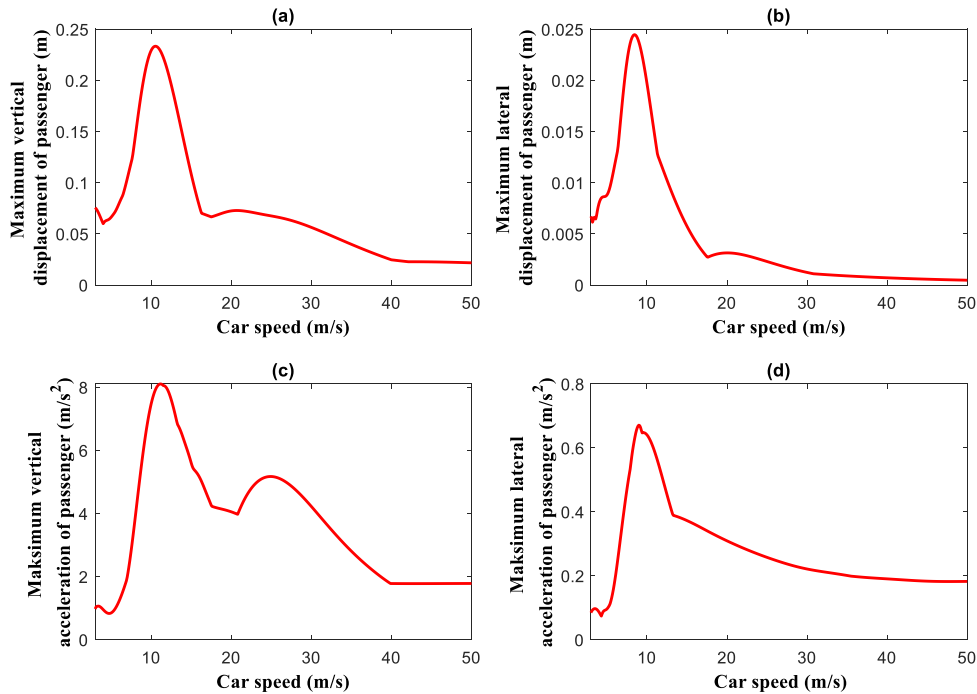


Figure 5 The effect of car speed on the maximum lateral and vertical dynamic responses of the passenger

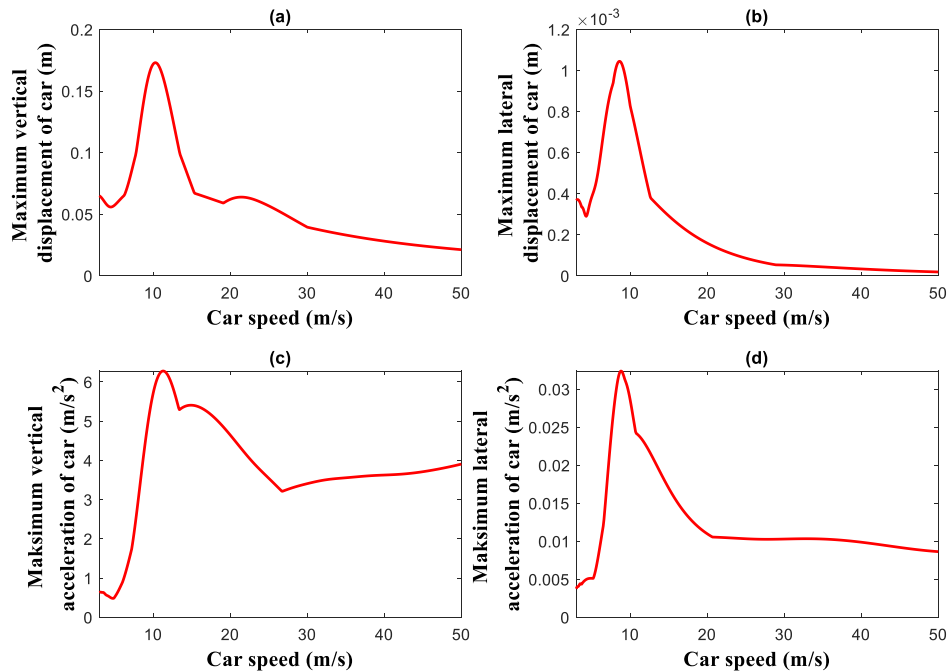


Figure 6 The effect of vehicle speed on the maximum lateral and vertical dynamic responses of the car

In Figure 7, the maximum pitch and roll movements are examined according to the speed of the car. While the roll response of the car increases until the car velocity is about 10 m/s, it is seen that the maximum roll motion decreases as the car velocity increase after this velocity. In Figures 7b and 7d, the car's maximum pitch motion occurred when the car velocity was 20 m/s.

4. CONCLUSION

In this study, lateral and vertical displacements and acceleration graphs of the full car model with fourteen degrees of freedom model with the passenger are given. In addition, the roll and pitch movements of the car were also examined. With the increase in the mass of the vehicle, the vertical displacements of the vehicle and the passenger decrease considerably, while the lateral displacement of the passenger almost does not change. However, the lateral displacement of the vehicle decreases as the mass increases. In addition, the vehicle's maximum dynamic response occurs when the car speed is approximately 10 m/s. Finally, The effect of car mass and car speed on these dynamic responses has been examined with graphics,

and as the car mass increases, the vertical displacement and acceleration values of the car decrease, while the damping of these values is delayed. At certain values of the car velocity, the car's maximum dynamic responses occur.

Acknowledgments

The authors would like to acknowledge the reviewers and editors of Sakarya University Journal of Science.

Funding

The author (s) has no received any financial support for the research, authorship or publication of this study.

The Declaration of Conflict of Interest/ Common Interest

No conflict of interest or common interest has been declared by the authors.

The Declaration of Ethics Committee Approval

This study does not require ethics committee permission or any special permission.

The Declaration of Research and Publication Ethics

The authors of the paper declare that they comply with the scientific, ethical and quotation rules of SAUJS in all processes of the paper and that they do not make any falsification on the data collected. In addition, they declare that Sakarya University Journal of Science and its editorial board have no responsibility for any ethical violations that may be encountered, and that this study has not been evaluated in any academic publication environment other than Sakarya University Journal of Science.

REFERENCES

- [1] A. Agharkakli, G.S. Sabet, A. Barouz, "Simulation and Analysis of Passive and Active Suspension System Using Quarter Car Model for Different Road Profile" *International Journal of Engineering Trends and Technology*, vol. 3, pp. 636–644, 2012.
- [2] M. Nagarkar, Y. Bhalerao, G.V. Patil, R.Z. Patil, "Multi-Objective Optimization of Nonlinear Quarter Car Suspension System - PID and LQR Control" *Procedia Manufacturing*, vol. 20, pp. 420–427, 2018.
- [3] E. Yildirim, I. Esen, "Dynamic Behavior and Force Analysis of the Full Vehicle Model using Newmark Average Acceleration Method" *Engineering, Technology & Applied Science Research*, vol. 10, pp. 5330–5339, 2020.
- [4] N. Yagiz, L.E. Sakman, R. Guclu, "Different control applications on a vehicle using fuzzy logic control" *Sadhana - Academy Proceedings in Engineering Sciences*, vol. 33, pp. 15–25, 2008.
- [5] M.M.M. Salem, A.A. Aly, "Fuzzy Control of a Quarter-Car Suspension System" *International Journal of Computer and Information Engineering*, vol. 3, pp. 1276–1281, 2009.
- [6] D. Singh, M.L. Aggarwal, "Passenger seat vibration control of a semi-active quarter car system with hybrid Fuzzy–PID approach" *International Journal of Dynamics and Control*, vol. 5, pp. 287–296, 2017.
- [7] D. Singh, "Self-Tuning Fuzzy Control of Seat Vibrations of Active Quarter Car Model" *International Journal of Computer and Systems Engineering*, vol. 11, pp. 1127–1133, 2017.
- [8] P. Swethamarai, P. Lakshmi, "Design and implementation of fuzzy-PID controller for an active quarter car driver model to minimize driver body acceleration" *IEEE International Systems Conference (SysCon)*, pp. 1–6, 2019.
- [9] M. Eroğlu, M.A. Koç, R. Kozan, İ. Esen, "Self-tuning fuzzy logic control of quarter car and bridge interaction model" *Sakarya University Journal of Science*, vol. 25, pp. 1197–1209, 2021.
- [10] M.A. Koç, "Analytic Method for Vibration Analysis of Track Structure Induced by High-Speed Train" *Sakarya University Journal of Science*, vol. 25, pp. 146–155, 2021.
- [11] C. Onat, S. Sivrioğlu, İ. Yüksek, "Bir Çeyrek Taşıt Modeli İçin H_{∞} Kontrolcü Tasarımı" *Mühendis ve Makine*, pp. 40–46, 2005.
- [12] M. Sever, H.S. Şendur, H. Yazıcı, M.S. Arslan, "Biodinamik sürücü modeli içeren bir taşıt süspansiyon sisteminin durum türevi geri beslemeli LQR ile aktif titreşim kontrolü" *Gazi Üniversitesi Mühendislik-Mimarlık Fakültesi Dergisi*, vol. 3, pp. 1573–1572, 2019.
- [13] C. Belgütay, " H_{∞} Control and Mathematical Modeling of A Quarter- Car System via Non-Parametric Approach" *Yıldız Technical University Graduate School of Natural and Applied Sciences*, 2015.
- [14] M.A. Koc, "Dynamic Response of an Euler-Bernoulli Beam Coupled with a Tuned Mass Damper under Moving Load Excitation" *Sakarya University Journal of Science ISSN*,

vol. 24, pp. 694–702, 2020.

- [15] C. Mizrak, I. Esen, "Determining Effects of Wagon Mass and Vehicle Velocity on Vertical Vibrations of a Rail Vehicle Moving with a Constant Acceleration on a Bridge Using Experimental and Numerical Methods", *Shock and Vibration*, 2015.